

# Alternation of [Ge<sub>5</sub>O<sub>11</sub>H]– Inorganic Sheets and Dabconium Cations in a Novel Layered Germanate: Catalytic Properties

C. Cascales, B. Gomez-Lor, E. Gutierrez-Puebla,\* M. Iglesias, M. A. Monge,\*  
C. Ruiz-Valero, and N. Snejko

*Instituto de Ciencia de Materiales de Madrid, CSIC Cantoblanco, E–28049 Madrid, Spain*

*Received July 4, 2001. Revised Manuscript Received September 14, 2001*

Ge<sub>5</sub>O<sub>11</sub>H[C<sub>6</sub>N<sub>2</sub>H<sub>13</sub>] has been hydrothermally synthesized. The structure of the material has been determined by single-crystal X-ray diffraction. This novel layered germanate consists of an alternation of [Ge<sub>5</sub>O<sub>11</sub>H]– inorganic sheets and monoprotonated 1,4-diazabicyclo-[2,2,2]-octane molecules. It exhibits an arrangement of 4- and 10-ring in infinite layers not observed before. The catalytic activity in Michael reactions has been tested showing that the addition occurs at the amine centers in the interlayer space. Reuse of the catalyst and the persistence of its structure after recovering has been proved.

## Introduction

The increasing demands of environmental legislation have induced the appearance of new catalysts and friendly catalytic processes, with an easy recovery and reuse of these materials. Zeolites have found many applications in fields of commercial importance, notably as catalysts, adsorbents, and ion exchangers. The choice of such inorganic oxide heterogenized catalysts is due to their well-defined porous structure, with apertures and cages of approximately the size of organic molecules. Properties such as shape selectivity, thermal stability, ease of separation from the products, and the possibility of regeneration of the deactivated catalysts, and their advantages in decreasing environmental problems, should also be mentioned.<sup>1–4</sup> Germanium porous materials offer great possibilities in the design of these demanded new open frameworks. The eventual coexistence of different coordination polyhedra around the Ge atom (tetrahedron, octahedron, and trigonal bipyramid) implies different charged frameworks. The magnitude of the M–O–M angle, which is smaller (120–135°) in germanates than in porous silicates (140–145°), allows the formation of different member rings into infinite layers unknown until now. And finally, the various ways in which these layers are joined led to different tunneled structures, all of them tridimensional.<sup>5–19</sup> Recently, Bu et al.<sup>20</sup> and Conradsson et al.<sup>21</sup> reported two layered

fluorogermanates, where the formation of the two-dimensional (2D) structure is favored in both cases by the presence of coordinated F atoms, and does not seem to be directly related to structure-directing agents used in the synthesis. In fact, the only interlayer species are inorganic cations.

In this article, we report the synthesis, structure, and thermal stability of a new germanate Ge<sub>5</sub>O<sub>11</sub>H [C<sub>6</sub>N<sub>2</sub>H<sub>13</sub>] (ICMM4) in whose synthesis the bulky directing agent, 1,4-diazabicyclo-[2,2,2]-octane (DABCO) prevents the formation of three-dimensional (3D) structure. We also present our findings on its application as a heterogeneous *green* and reusable catalyst in the Michael addition of nucleophiles to enones.

## Experimental Section

**Synthesis.** ICMM4 was synthesized hydrothermally, and variations in the procedure were explored, especially to avoid the presence of ASU-9,<sup>7</sup> a stable 3D germanate with AlPO<sub>4</sub>-16<sup>22</sup> topology, whose synthesis also involves DABCO (C<sub>6</sub>N<sub>2</sub>H<sub>12</sub>) among other organic templates. Finally, from a reaction

\* To whom correspondence should be addressed. E-mail: amonge@icmm.csic.es or egutierrez@icmm.csic.es

- (1) Corma, A. *Chem. Rev.* **1997**, *97*, 2373.
- (2) Cheetham, A. K.; Férey, G.; Loiseau, T. *Angew. Chem., Int. Ed. Engl.* **1999**, *38*, 3268.
- (3) Thomas, J. M. *Angew. Chem., Int. Ed. Engl.* **1999**, *38*, 3588.
- (4) Gier, T. E.; Bu, X.; Feng, P.; Stucky, G. D. *Nature (London)* **1998**, *395*, 154.
- (5) Cascales, C.; Gutiérrez-Puebla, E.; Monge, M. A.; Ruiz-Valero, C. *Angew. Chem.* **1998**, *110*, 135; *Angew. Chem., Int. Ed. Engl.* **1998**, *37*, 129.
- (6) Li, H.; Eddaoudi, M.; Richardson, D. A.; Yaghi, O. *J. Am. Chem. Soc.* **1998**, *120*, 8567.
- (7) Li, H.; Yaghi, O. *J. Am. Chem. Soc.* **1998**, *120*, 10569.
- (8) Bu, X.; Feng, P.; Stucky, G. D. *J. Am. Chem. Soc.* **1998**, *120*, 11204.

- (9) Bu, X.; Feng, P.; Gier, T. E.; Zhao, D.; Stucky, G. D. *J. Am. Chem. Soc.* **1998**, *120*, 13389.
- (10) Cascales, C.; Gutiérrez-Puebla, E.; Monge, M. A.; Ruiz-Valero, C. *Int. J. Inorg. Mater.* **1999**, *1*, 181.
- (11) Li, H.; Eddaoudi, M.; Yaghi, O. *Angew. Chem., Int. Ed. Engl.* **1999**, *38*, 653.
- (12) Cascales, C.; Gutiérrez-Puebla, E.; Iglesias, M.; Monge, M. A.; Ruiz-Valero, C. *Angew. Chem.* **1999**, *111*, 2592; *Angew. Chem., Int. Ed. Engl.* **1999**, *38*, 2436.
- (13) O'Keeffe, M.; Yaghi, O. *Chem. Eur. J.* **1999**, *5*, 2796.
- (14) Bu, X.; Feng, P.; Stucky, G. D. *Chem. Mater.* **2000**, *12*, 1811.
- (15) Li, J.; Ke, Y.; Zhang, Y.; He, G.; Jiang, Z.; Nishiura, M.; Imamoto, Y. *J. Am. Chem. Soc.* **2000**, *122*, 6110.
- (16) Cascales, C.; Gutiérrez-Puebla, E.; Iglesias, M.; Monge, M. A.; Ruiz-Valero, C.; Snejko, N. *Chem. Commun.* **2000**, 2145.
- (17) Conradsson, T.; Dadachov, M. S.; Zou, X. *Microporous Mesoporous Mater.* **2000**, *41*, 183.
- (18) Sun, K.; Dadachov, M. S.; Conradsson, T.; Zou, X. *Acta Crystallogr.* **2000**, *C56*, 1092.
- (19) Dadachov, M. S.; Sun, K.; Conradsson, T.; Zou, X. *Angew. Chem., Int. Ed. Engl.* **2000**, *39* (20), 3674.
- (20) Bu, X.; Feng, P.; Stucky, G. D. *Chem. Mater.* **1999**, *11*, 3423.
- (21) Conradsson, T.; Zou, X.; Dadachov, M. S. *Inorg. Chem.* **2000**, *39*, 1716.

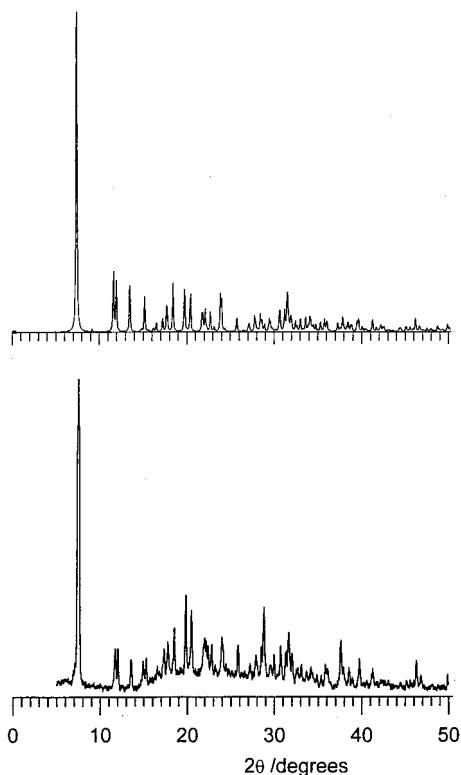


**Figure 1.** X-ray powder diagrams calculated for ICMM4,  $\text{Ge}_5\text{O}_{11}\text{H}[\text{C}_6\text{N}_2\text{H}_{13}]$  from single-crystal structure data (top); recorded for the obtained material (bottom).

mixture containing  $\text{GeO}_2$ , DABCO, and  $\text{H}_2\text{O}$  in molar ratios 1:2:15 (pH = 10.8), introduced and sealed in a Teflon-lined stainless autoclave and heated at 170 °C for 7 days, ICMM4 was obtained as the sole product of the reaction. Purity of the resulting solid product was checked by X-ray powder diffraction. Figure 1 shows the comparison between the X-ray powder diffraction patterns of both the experimental and the calculated single-crystal structure data.

**X-ray Structure Determination.** A very small crystal of this compound was selected and mounted in a Bruker Smart CCD diffractometer equipped with a normal-focus, 2.4-kw sealed tube X-ray source operating at 50 kV and 20 mA. Data were collected at room temperature over a hemisphere of reciprocal space by a combination of three frame sets. The crystal-to-detector distance was 5.02 cm. Unit cell dimensions were determined by a least-squares fit of all collected reflections. Each set exposure time was of 20 s covering 0.3° in  $\omega$ . The first 50 frames of data were recollected at the end of the data collection to monitor crystal decay. The structure was solved by direct methods. The hydrogen atoms of the OH group and the protonated amine were located in difference Fourier maps and isotropically refined, the remaining being geometrically situated. Mixed full-matrix least-squares refinement was performed. Some small disorder from the thermal motion involved the DABCO molecules; consequently, three of their C atoms were isotropically refined. Maximum residual electron densities are very close to the germanium atoms. A summary of the fundamental crystal and refinement data is given in Table 1. Most of the calculations were performed with SMART<sup>23</sup> software, for data collection and data reduction, and SHELXTL.<sup>24</sup>

**X-ray Powder Diffraction.** The X-ray powder diffraction patterns were taken at room temperature by using a Siemens

**Table 1. Crystal Data and Structure Refinement for  $\text{Ge}_5\text{O}_{11}\text{H}[\text{C}_6\text{N}_2\text{H}_{13}]$**

empirical formula	$\text{Ge}_5\text{O}_{11}\text{H}[\text{C}_6\text{N}_2\text{H}_{13}]$
formula weight	1306.28
temperature	296 (2) K
wavelength	0.71073 Å
crystal system	triclinic
space group	<i>P</i> 1
unit cell dimensions	$a = 6.575(1)$ Å $\alpha = 91.594(4)^\circ$ $b = 9.650(2)$ Å $\beta = 91.863(4)^\circ$ $c = 11.988$ Å $\gamma = 91.217(4)^\circ$
volume, <i>Z</i>	759.6(2) Å <sup>3</sup> , 1
density (calculate)	2.855 Mg/m <sup>3</sup>
absorption coefficient	9.840 mm <sup>-1</sup>
<i>F</i> (000)	624
crystal size	0.04 × 0.04 × 0.02 mm
Θ range for data collection	2.67–24.74°
limiting indices	(–7, –11, –9) (7, 11, 14)
reflections collected	3692
independent reflections	2372 ( $R_{\text{int}} = 0.0571$ )
absorption correction	sadabs
max. and min. transmission	0.48 and 0.69
refinement method	full-matrix least-squares on $F^2$
data/restraints/parameters	2372/0/205
goodness-of-fit on $F^2$	0.902
final <i>R</i> indices [ $I > 2\sigma(I)$ ]	$R_1 = 0.0587$ , $wR_2 = 0.1302$
<i>R</i> indices (all data)	$R_1 = 0.0981$ , $wR_2 = 0.1466$
largest diff. peak and hole	1.847 and –1.035 eÅ <sup>-3</sup>

D-500 diffractometer in the step scan mode,  $\text{CuK}\alpha$  ( $\lambda = 1.540598$  Å) radiation, at a step value of 0.02°, measuring for 10 s at each step.

**Catalytic Reactions.** In a standard experiment acrolein (1 mmol) and nitroethane (2 mmol) were added to a suspension of the as synthesized catalyst (10 mol %) in dry toluene (5 mL). The mixture was stirred at 60 °C and monitored by gas chromatography (GC) with undecane as internal standard. GC analysis was performed using a Hewlett-Packard 5890 II with a flame ionization detector in cross-linked methylsilicone or heptaquis-(6-*tert*-butyl-dimethylsilyl)-2,3-dipentyl)- $\beta$ -cyclodextrin/methylsilicone columns.

## Results and Discussion

According to the crystal structure determination, the composition of the obtained material is  $\text{Ge}_5\text{O}_{11}\text{H}[\text{C}_6\text{N}_2\text{H}_{13}]$ . Final atomic coordinates and selected bond distances and angles are given in Tables 2 and 3, respectively. Figure 2 is an ORTEP drawing of the asymmetric unit. In this compound four Ge atoms are tetrahedrally coordinated to oxygen [range of Ge–O bond lengths, 1.708(9)–1.783(11) Å; O–Ge–O bond angles, 101.0(5)–119.0(5)°; Ge–O–Ge, 120.6(6)–130.4(6)°], and one, Ge(2), is pentacoordinated forming a trigonal bipyramid [range of Ge–O bond lengths, 1.755(9)–1.900(10) Å; O–Ge–O bond angles, 85.9(4)–172.3(4)°; Ge–O–Ge, 120.6(6)–136.1(6)°], in agreement with those observed for other pentacoordinated germanates.<sup>25</sup>

Tetrahedra are linked among them by vertex sharing forming  $\text{Ge}_4\text{O}_8$  tetrameric units. These units are joined in the *a* direction giving rise to infinite chains. Note the very important role played by the  $\text{GeO}_5$  trigonal bipyramid in the building of both the single (L) and the double layer or block (B) (Figure 3). Along the *b* direction, the chains are joined through the bipyramid apical oxygen atoms to form 4- and 10-polyhedra ring sheets (L) (Figure 4). This arrangement had not been observed before in any microporous germanate, because the 3- to 9-ring association seems to be more fre-

(22) O'Keeffe, M.; Hyde, B. G. *Crystal Structures: I. Patterns and Symmetry*; Mineralogical Society of America: Washington, DC, 1996.

(23) *Software for the SMART System*. Siemens Analytical X-ray Instruments Inc.: Madison, WI, 1995.

(24) *SHELXTL™*, Version 5.0; Siemens Analytical X-ray Instruments Inc.: Madison, WI, 1995.

(25) Zhou, Y.; Zhu, H.; Chen, Z.; Chen, M.; Xu, Y.; Zhang, H.; Zhao, D. *Angew. Chem., Int. Ed. Engl.* **2001**, *40*, 2166.

**Table 2. Atomic Coordinates and Equivalent Isotropic Displacement Parameters for Ge<sub>5</sub>O<sub>11</sub>H[C<sub>6</sub>N<sub>2</sub>H<sub>13</sub>]**

atom	X	Y	Z	$U_{eq}^a$
Ge1	0.1491(2)	0.4320(2)	0.6404(1)	9(1)
Ge2	-0.1262(2)	0.2612(2)	0.4617(1)	9(1)
Ge3	0.0928(2)	-0.2295(2)	0.2057(1)	12(1)
Ge4	0.5168(2)	0.2291(2)	0.6361(1)	10(1)
Ge5	-0.1195(2)	-0.0381(2)	0.3728(1)	13(1)
O1	0.360(1)	0.090(1)	0.5876(9)	17(2)
O2	-0.040(1)	0.389(1)	0.7330(9)	18(2)
O3	-0.360(1)	0.297(1)	0.5238(9)	16(2)
O4	0.337(1)	-0.175(1)	0.2490(8)	9(2)
O5	-0.086(1)	0.111(1)	0.5588(9)	19(3)
O6	0.182(1)	0.6081(9)	0.6477(8)	12(2)
O7	-0.116(1)	0.139(1)	0.3493(8)	14(2)
O8	-0.093(1)	-0.106(1)	0.2345(9)	18(2)
O9	0.372(1)	0.363(1)	0.6947(8)	15(2)
O10	0.093(1)	0.355(1)	0.5094(8)	13(2)
O11	0.107(2)	-0.252(1)	0.0620(9)	21(3)
N1	0.478(2)	0.731(2)	0.788(1)	46(5)
N2	0.765(2)	0.758(1)	0.936(1)	18(3)
C1	0.660(7)	0.885(5)	0.926(4)	17(2)
C2	0.431(4)	0.646(3)	0.880(2)	8(1)
C3	0.607(4)	0.664(4)	0.966(2)	14(2)
C4	0.458(6)	0.877(4)	0.850(4)	14(1)
C5	0.831(6)	0.728(4)	0.833(3)	14(1)
C6	0.661(7)	0.705(5)	0.742(4)	16(2)

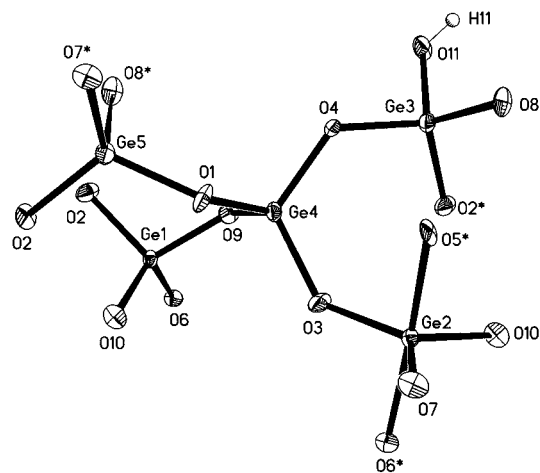
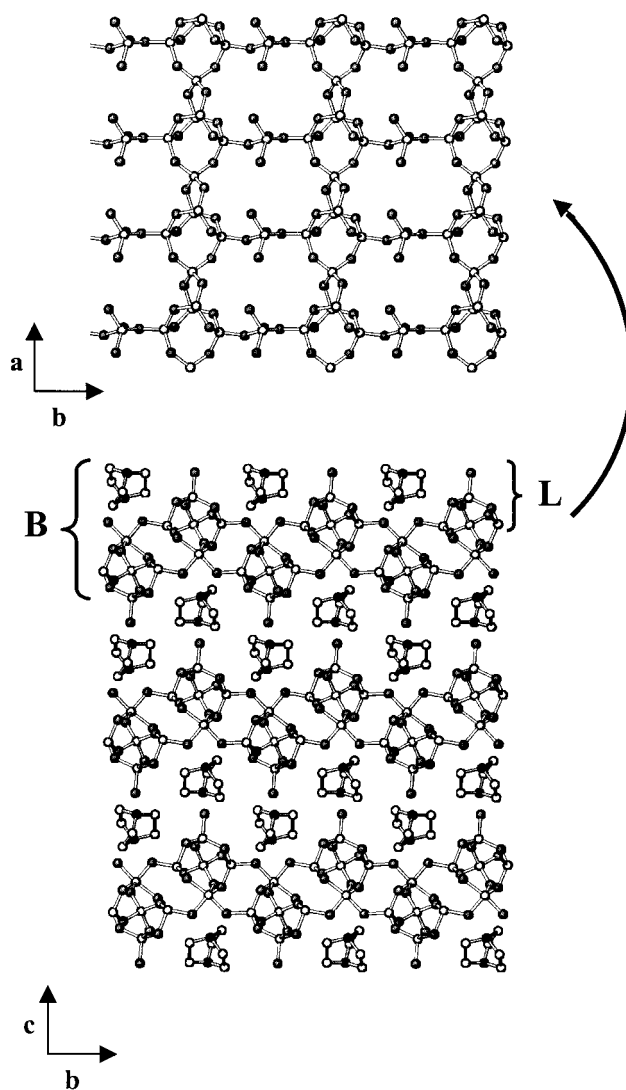
<sup>a</sup>  $U_{eq}$  ( $\text{\AA}^2 \cdot 10^3$ ) is defined as third of the trace of the orthogonalized  $U_{ij}$  tensor.

**Table 3. Selected Bond Lengths ( $\text{\AA}$ ) and Angles ( $^\circ$ ) for Ge<sub>5</sub>O<sub>11</sub>H[C<sub>6</sub>N<sub>2</sub>H<sub>13</sub>]**

Ge1—O2	1.744(10)	Ge4—O4 <sup>a</sup>	1.752(9)
Ge1—O6	1.708(9)	Ge4—O8	1.765(10)
Ge1—O8	1.738(10)	Ge5—O1 <sup>b</sup>	1.734(9)
Ge1—O10	1.745(10)	Ge5—O5 <sup>b</sup>	1.732(9)
Ge2—O3	1.763(10)	Ge5—O7	1.740(9)
Ge2—O5	1.900(10)	Ge5—O8	1.783(11)
Ge2—O6 <sup>c</sup>	1.877(9)	N1—C2	1.43(3)
Ge2—O7	1.770(10)	N1—C4	1.58(4)
Ge2—O10	1.755(9)	N1—C6	1.36(5)
Ge3—O2 <sup>b</sup>	1.761(10)	N2—C1	1.43(4)
Ge3—O4	1.740(9)	N2—C3	1.42(3)
Ge3—O8	1.758(9)	N2—C5	1.35(4)
Ge3—O11	1.736(11)	C1—C4	1.58(5)
Ge4—O1	1.749(10)	C2—C3	1.53(3)
Ge4—O3 <sup>d</sup>	1.730(10)	C5—C6	1.54(5)
O2—Ge1—O6	107.1(5)	O2 <sup>b</sup> —Ge3—O8	112.1(4)
O2—Ge1—O8	106.0(4)	O2 <sup>b</sup> —Ge3—O11	110.2(6)
O2—Ge1—O10	110.1(5)	O4—Ge3—O8	113.2(5)
O6—Ge1—O8	106.5(5)	O4—Ge3—O11	104.0(5)
O6—Ge1—O10	117.5(5)	O8—Ge3—O11	108.8(5)
O8—Ge1—O10	109.0(5)	O1—Ge4—O3 <sup>d</sup>	108.5(5)
O3—Ge2—O5	90.2(4)	O1—Ge4—O4 <sup>a</sup>	108.3(5)
O3—Ge2—O6 <sup>c</sup>	90.2(3)	O1—Ge4—O8	111.2(5)
O3—Ge2—O7	120.5(5)	O3 <sup>d</sup> —Ge4—O4 <sup>a</sup>	118.8(4)
O3—Ge2—O10	118.7(5)	O3 <sup>d</sup> —Ge4—O8	107.3(4)
O5—Ge2—O6 <sup>c</sup>	172.3(4)	O4 <sup>a</sup> —Ge4—O8	102.7(5)
O5—Ge2—O7	87.3(5)	O1 <sup>b</sup> —Ge5—O5 <sup>b</sup>	117.1(5)
O5—Ge2—O10	95.0(4)	O1 <sup>b</sup> —Ge5—O7	109.6(5)
O6 <sup>c</sup> —Ge2—O7	85.9(4)	O1 <sup>b</sup> —Ge5—O8	106.0(5)
O6 <sup>c</sup> —Ge2—O10	91.5(4)	O5 <sup>b</sup> —Ge5—O7	119.5(5)
O7—Ge2—O10	120.7(4)	O5 <sup>b</sup> —Ge5—O8	101.0(5)
O2 <sup>b</sup> —Ge3—O4	108.2(5)	O7—Ge5—O8	100.9(5)

Symmetry transformations used to generate equivalent atoms: <sup>a</sup>  $(-x+1, -y, -z+1)$  <sup>b</sup>  $(-x, -y, -z+1)$  <sup>c</sup>  $(-x, -y+1, -z+1)$  <sup>d</sup>  $(x+1, y, z)$

quent.<sup>5,10,12,16</sup> Every two of these described layers join each other, in the alternated configuration, via the three axial oxygen atoms of the GeO<sub>5</sub> trigonal bipyramids. These connections give rise to a kind of 4 = 1 secondary structural building unit (SBU) in which the bridging germanium is coordinated to five oxygen atoms. Thus, the double layer, or block B, can be depicted in terms of

**Figure 2.** Labeled ORTEP plot of ICMM4 showing more than the asymmetric unit. \* indicates atoms symmetrically related.**Figure 3.** Polyhedral representation of the structure. The GeO<sub>5</sub> environment is represented by sticks and balls.

infinite 4 = 1 SBU joined among them through oxygen atoms belonging to the trigonal bipyramid. The only oxygen atom, O(11), that is not involved in connectivity inside the block belongs to a coordinated hydroxyl group and is pointing outside the block, toward the interblock space. The presence of this OH group is confirmed by

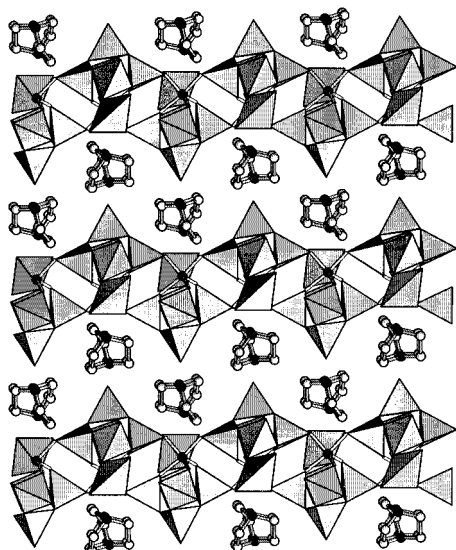


**Figure 4.** View of the structure of ICMM4 along the [001] direction showing the blocks B and the layers L (grey spheres, Ge and C; black, O and N). (top) detail of the 4- and 10-ring layer (L).

the appearance of a band at  $3385\text{ cm}^{-1}$  in the expected range for  $\nu_{\text{O-H}}$  stretching frequencies. Along the  $c$  direction, infinite blocks of  $[\text{Ge}_5\text{O}_{11}\text{H}]^-$  composition alternate with monoprotonated Dabconium cations  $[\text{C}_6\text{N}_2\text{H}_{13}]^+$  (Figures 3 and 4). Hydrogen atoms of both the OH group and protonated DABCO were located in a difference Fourier synthesis and isotropically refined. There are two hydrogen bonds per formula between the inorganic blocks and the organic molecule. The OH group of one block is bonded to the nonprotonated nitrogen atom, N(2), of DABCO, and that protonated, N(1), to one oxygen atom O(6) belonging to another block framework. The involved lengths in angstroms are: O11-H, 0.8(2); O11...N2, 2.67(3); H11...N2, 2.30(8); and N1-H, 1.0(1); N1...O6, 2.76(4); H1...O6, 1.78(8), respectively.

In our previously reported germanium zeotypes ICMM2<sup>12</sup> and ICMM3,<sup>16</sup> the cohesion between blocks along the stacking direction is established through the only oxygen atoms not involved in connectivity inside the double layers. These Ge-O-Ge bonds give rise to 3D structures, which contain intersecting tunnels along the three directions. On the contrary, in the novel 2D ICMM4 these interblock connections have been avoided by stabilizing, via synthesis, a voluminous organic molecule in the interlayer space. Although DABCO is involved in the synthesis of several 3D tunneled germanium zeotypes, such as ASU-97 or ICMM5,<sup>26</sup> the synthesis conditions of the new ICMM4 are quite different. The procedure was used to avoid several simultaneously acting templates. The only difference between the synthesis of the 3D ICMM3 and that of the new ICMM4 is the use in the later of a bulkier amine as template, which resulted in the 2D ICMM4.

Thermogravimetric and differential thermal analyses in static air show that the compound is stable up to 250 °C. Then, a progressive weight loss of 20.5% is observed between 250 and 450 °C, accompanied by an endothermic effect corresponding to the loss of the DABCO

(26) Medina, M.E.; Iglesias, M.; Monge, M. A.; Gutierrez-Puebla, E., unpublished results.

**Scheme 1**

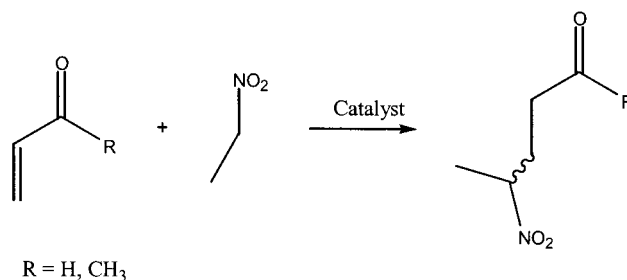


**Table 4.** Influence of the Temperature on Reactivity for the Addition of Nitroethane to Acrolein

$T$ (K)	conversion (%)
323	28; 51 <sup>a</sup>
313	18
273	15; 28 <sup>a</sup>

<sup>a</sup> Reactions were performed with a 40% molar of catalyst.

**Table 5.** Results of Michael Addition with Nitroethane Using ICMM4 as Catalyst

substrate	catalyst (%)	time (h)	conversion (%)
acrolein	10	5	33
acrolein	20	2	27
acrolein	40	1	51
methyl vinyl ketone	10	20	30

Reactions performed on 1 mmol of enone and 2 mmol of nitroethane in 5 mL of dry toluene at 323 K.

**Table 6.** Activity of the ICMM4 Recovered Catalyst in Michael Addition Reaction

run	conversion (%)
1	33
2	28
3	31
4	30

molecule and one water molecule. X-ray powder diffraction indicates that at 450 °C the final product is crystalline germanium dioxide.

**Catalytic Properties.** The Michael addition of nucleophiles to enones catalyzed by amines or alkaline alkoxides have been extensively studied<sup>27,28</sup> and applied for preparation of several valuable intermediates in organic chemistry.<sup>29,30</sup> The new heterogeneous catalyst ICMM4 has been tested in the addition of nitroalkanes to enones (Scheme 1). The reaction affords 4-nitropentanal and 5-nitro-2-hexanone. The results obtained in the evolution of the reaction were monitored by GC and the product was isolated by filtration of the catalyst; after normal workup the yield was, as expected, 8–10% lower than that given by GC.

The influence of the temperature, framework topology, and size of reactants in the reaction was studied. Results are given in Tables 4 and 5.

The ICMM4-catalyzed addition of nitroethane to enones was used to examine the effects of different temperatures on chemical yield. The reactivity increases

(27) Jong, J. C.; Berg, K. J.; Leusen, A. M.; Feringa, B. L. *Tetrahedron Lett.* 1988, 44, 721.

(28) Fariña, F.; Maestro, M. C.; Martín, M. R.; Martín, M. V.; Sánchez, F. *Heterocycles* 1983, 20, 1761.

(29) Feringa, B. L.; Jong, J. C. *Bull. Soc. Chim. Belg.* 1992, 101, 627.

(30) d'Angelo, J.; Cave, C.; Desmaele, D.; Dumas, F. *Trends Org. Chem.* 1993, 4, 55.

with the temperature in the range 298–323 K for both substrates. Lower temperatures require a longer reaction time and a higher catalyst/substrate ratio to reach reasonable chemical yields.

The reaction rate decreased when bulkier reagents were used. The reaction with methyl vinyl ketone was slow, and conversions up to 30% were obtained only after 24 h. This difference of operativeness of the catalyst evidences the lack of accessibility of the reactants to the basic centers, and thus the occurrence of the reaction in the interlayer space. A series of blank experiments revealed that each component is essential for an effective catalytic reaction and the system is relatively unaffected by changing the order of mixing.

Finally, evidence of the ICMM4 catalyst recycling is shown in Table 6. The filtered and dried recovered material promotes the Michael addition more than four times.

In conclusion, the structural original features of the novel Ge<sub>5</sub>O<sub>11</sub>H[C<sub>6</sub>N<sub>2</sub>H<sub>13</sub>] are: the arrangement of 4- and 10-polyhedra-ring-containing sheets not previously observed, and the alternation of inorganic Ge<sub>5</sub>O<sub>11</sub>H<sup>-</sup> sheets and Dabconium cations. This last fact allows unhindered accessibility of the reactants to the basic centers situated in the interlayer space.

This material can be considered a practical alternative to soluble base catalysts because of the following advantages: good stability, high activity under mild conditions, possibility of free election of solvent, easy separation and reuse along with waste minimization.

**Acknowledgment.** This work has been supported by the Spanish CICYT MAT1999-0892 and DGEISIC PB97-1200.

CM011169U